

# First observation of the $\beta 3\alpha p$ decay of $^{13}\text{O}$ via $\beta$ -delayed charged-particle spectroscopy

J. Bishop,<sup>1</sup> G.V. Rogachev,<sup>1,2,3</sup> S. Ahn,<sup>4</sup> M. Barbui,<sup>1</sup> S.M. Cha,<sup>4</sup> E. Harris,<sup>1,2</sup> C. Hunt,<sup>1,2</sup>  
C.H. Kim,<sup>5</sup> D. Kim,<sup>4</sup> S.H. Kim,<sup>6</sup> E. Koshchiy,<sup>1</sup> Z. Luo,<sup>1,2</sup> C. Park,<sup>4</sup> C.E. Parker,<sup>1</sup>  
E.C. Pollacco,<sup>7</sup> B.T. Roeder,<sup>1</sup> M. Roosa,<sup>1,2</sup> A. Saastamoinen,<sup>1</sup> and D.P. Scriven<sup>1,2</sup>

<sup>1</sup>*Cyclotron Institute, Texas A&M University, College Station, TX 77843, USA*

<sup>2</sup>*Department of Physics & Astronomy, Texas A&M University, College Station, TX 77843, USA*

<sup>3</sup>*Nuclear Solutions Institute, Texas A&M University, College Station, TX 77843, USA*

<sup>4</sup>*Center for Exotic Nuclear Studies, Institute for Basic Science, 34126 Daejeon, Republic of Korea*

<sup>5</sup>*Department of Physics, Sungkyunkwan University (SKKU), Republic of Korea*

<sup>6</sup>*Department of Physics, Sungkyunkwan University, Suwon 16419, Republic of Korea*

<sup>7</sup>*IRFU, CEA, Université Paris-Saclay, Gif-Sur-Yvette, France*

(Dated: March 1, 2023)

**Background:** The  $\beta$ -delayed proton-decay of  $^{13}\text{O}$  has previously been studied, but the direct observation of  $\beta$ -delayed  $3\alpha p$  decay has not been reported.

**Purpose:** Rare  $3\alpha p$  events from the decay of excited states in  $^{13}\text{N}^*$  provide a sensitive probe of cluster configurations in  $^{13}\text{N}$ .

**Method:** To measure the low-energy products following  $\beta$ -delayed  $3\alpha p$ -decay, the TexAT Time Projection Chamber was employed using the one-at-a-time  $\beta$ -delayed charged-particle spectroscopy technique at the Cyclotron Institute, Texas A&M University.

**Results:** A total of  $1.9 \times 10^5$   $^{13}\text{O}$  implantations were made inside the TexAT Time Projection Chamber. 149  $3\alpha p$  events were observed yielding a  $\beta$ -delayed  $3\alpha p$  branching ratio of 0.078(6)%.

**Conclusion:** Four previously unknown  $\alpha$ -decaying excited states were observed in  $^{13}\text{N}$  at 11.3 MeV, 12.4 MeV, 13.1 MeV and 13.7 MeV and the decay modes for these states were established. We demonstrate that clustering must dominate the structure of these states to exhibit the observed decay branching ratios.

## I. INTRODUCTION

Exotic neutron-deficient nuclei provide an excellent opportunity to explore new decay modes. Large  $\beta$ -decay  $Q$ -values make it possible to populate proton- or  $\alpha$ -unbound states in daughter nuclei, paving the way for observation of  $\beta$ -delayed charged-particle emissions. Reviews of advances in  $\beta$ -delayed charged-particle emission studies can be found in Ref. [1, 2], where  $\beta$ -delayed one, two, and three proton decays as well as  $\alpha p/p\alpha$  decays are discussed. Here we report on a new decay mode that has not been observed before, the  $\beta 3\alpha p$ . Not only do we identify these exotic decays of  $^{13}\text{O}$ , but we were also able to use it to obtain information on cluster structure in excited states of the daughter nucleus,  $^{13}\text{N}$ .

Clustering phenomena are prevalent in light nuclei and are an excellent test ground for understanding few-body systems that are theoretically accessible. These clustering phenomena have been well-studied in  $\alpha$ -conjugate nuclei. Much less experimental information is available for  $N \neq Z$  nuclei. Yet, theoretical studies (e.g. [3–5]) indicate that cluster configurations may be even richer in non-self-conjugate nuclei, opening a window of opportunity to confront the highly-non-trivial theoretical predictions with experimental data. Recent experimental studies of clustering in non-self-conjugate nuclei already produced exciting results, such as hints for linear chain structures stabilized by “extra” nucleons (e.g. [6–8]) and indications for super-radiance [9, 10].

Of particular interest is the nucleus  $^{13}\text{N}$  where three

$\alpha$  clusters and an “extra” proton can form exotic cluster configurations. Resonant  $^9\text{B} + \alpha$  scattering or  $\alpha$ -transfer reactions are not possible because  $^9\text{B}$  is proton unbound with a half life of the order of  $10^{-18}$  s. Instead, one may use  $\beta$ -delayed charged-particle spectroscopy to populate states in  $^{13}\text{N}$  via  $^{13}\text{O}$  and observe the decays to a final state of  $3\alpha p$ . The  $\beta$ -delayed proton channel has previously been studied for  $^{13}\text{O}$  [11] where limited statistics showed only a very small sensitivity to populating the  $p + ^{12}\text{C}(0_2^+)$  (Hoyle state) which results in a  $3\alpha + p$  final state. Utilizing the Texas Active Target (TexAT) Time Projection Chamber to perform one-at-a-time  $\beta$ -delayed charged-particle spectroscopy,  $\alpha$ -decays from the near  $\alpha$ -threshold excited states in  $^{13}\text{N}$  have been observed for the first time, providing insights into the  $\alpha + ^9\text{B}$  clustering. Capitalizing on the advantages of TPCs for  $\beta$ -delayed charged-particle emission studies, unambiguous and background-free identifications of the  $\beta 3\alpha p$  events were made. Reconstruction of complete kinematics for these exotic decays allowed for robust decay channel assignments, providing insights into the cluster structure of the  $^{13}\text{N}$  excited states. Evidence for the  $\frac{1}{2}^+$  first excited state in  $^9\text{B}$ , mirror of the well-known  $\frac{1}{2}^+$  in  $^9\text{Be}$ , was an unexpected byproduct of these measurements, demonstrating the sensitivity of the technique.

## II. EXPERIMENTAL SETUP

The  $\beta$ -delayed charged-particle spectroscopy technique with the TexAT TPC has previously been applied for  $\beta$ -delayed  $3\alpha$  decay studies of  $^{12}\text{N}$  via  $^{12}\text{C}^*$  [12]. A detailed description of the technique is provided in [13]. Here, we utilize the same experimental approach to observe the  $\beta$ -delayed  $3\alpha$  decays of  $^{13}\text{O}$  via  $^{13}\text{N}^*$ . We implant  $\beta$ -decaying  $^{13}\text{O}$  one-at-a-time into the TexAT TPC by providing a phase shift signal to the K500 Cyclotron at Texas A&M University when a successful implantation has taken place to halt the primary beam. This phase shift then lasts for three half-lives or until the observation of a  $\beta$ -delayed charged particle in TexAT, with the DAQ ready to accept the trigger. The phase shift is then reset to allow for the next implantation. A beam of  $^{13}\text{O}$  was produced via the  $^3\text{He}(^{14}\text{N}, ^{13}\text{O})$  reaction at the MARS (Momentum Achromat Recoil Separator) [14] with a typical intensity of 5 pps with an energy of 15.1 MeV/u, degraded by an aluminum foil to 2 MeV/u, to stop inside of the TexAT sensitive area, filled with 50 Torr of  $\text{CO}_2$  gas. To measure the correlated implantation/decay events, the 2p trigger mode of GET electronics [15] was employed where the occurrence of two triggers within a 30 ms time window was required for a full event. The first trigger, the L1A (implantation), is generated if the Micromegas pad multiplicity exceeds 10. If, during the 30 ms following the L1A trigger, another trigger occurs with Micromegas pad multiplicity above two, the second L1B (decay) trigger event and the time between the L1A and L1B are recorded. For normalization and beam characterization, all events where recorder, even if L1B trigger never came.

## III. ANALYSIS

The complete L1A (implant) + L1B (decay) events were selected with the time between the two triggers in the range of 1-30 ms. The short times ( $<1$  ms) were omitted to remove double trigger events due to sudden beam-induced noise. To ensure the implanted ion is  $^{13}\text{O}$ , the energy deposited by the beam implant event in the Micromegas “Jr” (MM Jr) beam tracker [16] at the entrance to the TexAT chamber was recorded. The beam contaminants were  $^7\text{Be}$  and  $^{10}\text{C}$ , dominated by  $^7\text{Be}$  at  $\approx 28\%$  of the beam intensity.

Following an identification of  $^{13}\text{O}$  implant, the stopping position was evaluated event-by-event using implant tracks, selecting only those which stopped inside the active area of the Micromegas and not closer than 31.5 mm from the edge. The spread of the  $^{13}\text{O}$  stopping position inside TexAT was 67.5 mm due to straggling.

Further selection was performed by imposing tight correlation ( $<5$  mm) between the  $^{13}\text{O}$  stopping location and the vertex location of the respective decay event. Events which passed this test were then fit with a single track segment using a randomly-sampled  $\chi$ -squared minimiza-

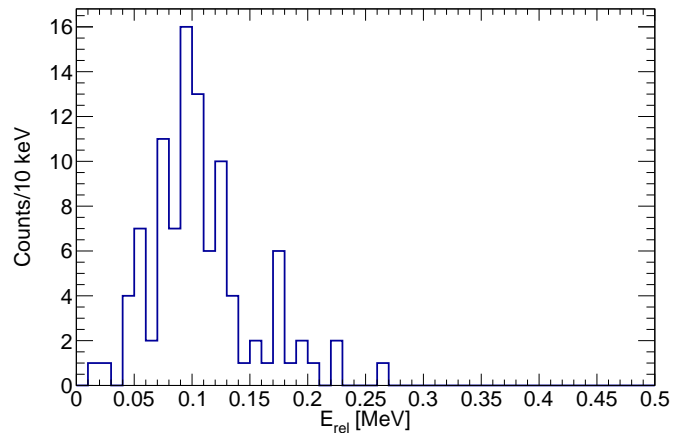


FIG. 1. Relative energy spectrum for pairs of  $\alpha$ -particles with the smallest relative energy of the three  $\alpha$ -tracks. The  $^8\text{Be}(g.s)$  at 92 keV is well-reproduced.

tion algorithm. If good fit is achieved, these events were identified as single proton events. The  $\beta$ -delayed proton spectrum replicates the previous results [11] well, albeit with decreased resolution. The remaining events were fit with four track segments as candidates for  $\beta 3\alpha$  decay using randomly-sampled  $\chi$ -squared minimization. They were then inspected visually to evaluate the fits’ quality. Given the complexity of the fits, manual modifications of the fit algorithm parameters were required for some events.

## IV. $3\alpha$ +PROTON EVENTS

Overall, 149  $\beta 3\alpha$  events were identified. Due to the size of the TPC and limitations on reconstruction in parts of the TexAT TPC, only 102 out of 149 of these events allow for complete reconstruction. The “incomplete” events are dominated by the  $^9\text{B}(g.s.)+\alpha$  decay as this produces a high-energy  $\alpha$ -particle that may escape from the active volume of the TexAT TPC. The efficiency for the  $\alpha_0$  decay starts to deviate from 100% at  $E_x = 10$  MeV, slowly drops to around 60% at  $E_x = 14$  MeV. The efficiency for  $\alpha_1$  and  $\alpha_3$  are less affected and only decrease to 70% at  $E_x = 14$  MeV. In proton decays to the Hoyle state, most of the energy is taken by protons and the resulting three  $\alpha$ -tracks of the pre-selected events are always confined to the active volume of the TPC. Proton tracks were not required in reconstruction as complete kinematics can be recovered from the remaining three  $\alpha$ -tracks. Therefore, there was no efficiency reduction for the  $p+^{12}\text{C}(\text{Hoyle})$  decays. The yields given in Table I are corrected for these experimental effects.

In order to identify the parent state in  $^{13}\text{N}^*$ , the lowest energy deposition arm was identified as the proton track and the momentum of the 3  $\alpha$ -particles was determined by the length and direction of  $\alpha$ -tracks in the

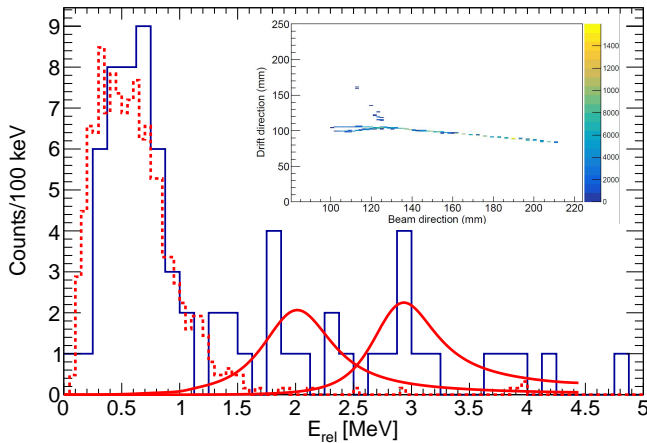


FIG. 2. For events that do not decay via the Hoyle state, the relative energy spectrum is shown here which is generated by selecting the two  $\alpha$ -particles that produce the  ${}^8\text{Be}(g.s)$  and then reconstructing the  ${}^9\text{B}$  relative energy with the proton. Overlaid in dashed red are simulated data for the ground state contribution and in solid red are the  $\frac{1}{2}^+$  and  $\frac{5}{2}^+$  states from single channel R-Matrix calculations convoluted with a Gaussian with  $\sigma = 0.23$  MeV. The  $\frac{1}{2}^+$  parameters are those obtained by Wheldon [17] which show excellent agreement. Inset: projection of an example  $\alpha+{}^9\text{B}(g.s)$  event in the TPC with the color indicating energy deposition. The lower energy deposition proton can be seen extending upwards and then escapes the TPC active area.

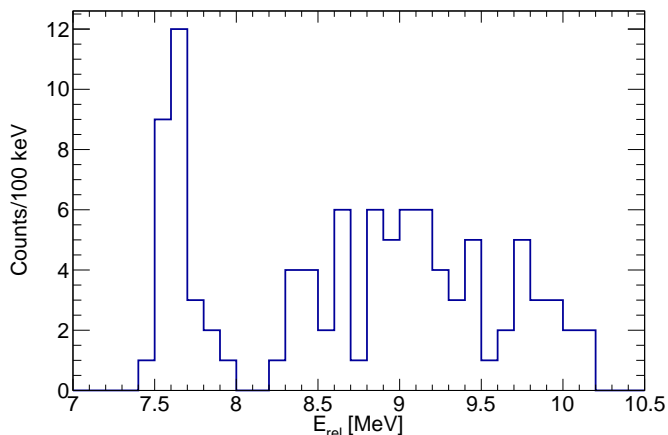


FIG. 3. Invariant mass spectrum for  ${}^{12}\text{C}$  from  $3\alpha$ -particles. A peak at 7.65 MeV is seen, well reproducing the Hoyle state energy and a broad peak is seen at higher excitation energies which correspond to events that decay via  ${}^9\text{B} + \alpha$ .

gas. Protons almost always escape the sensitive volume, and the proton momentum is reconstructed from momentum conservation. The decay energy is then the sum of the three  $\alpha$ -particles' and proton energy. From here, the  ${}^8\text{Be}$  (Fig. 1),  ${}^9\text{B}$  (Fig. 2) and  ${}^{12}\text{C}$  (Fig. 3) excitation energies were determined from the invariant mass. This allowed for a selection of events which proceeded to de-

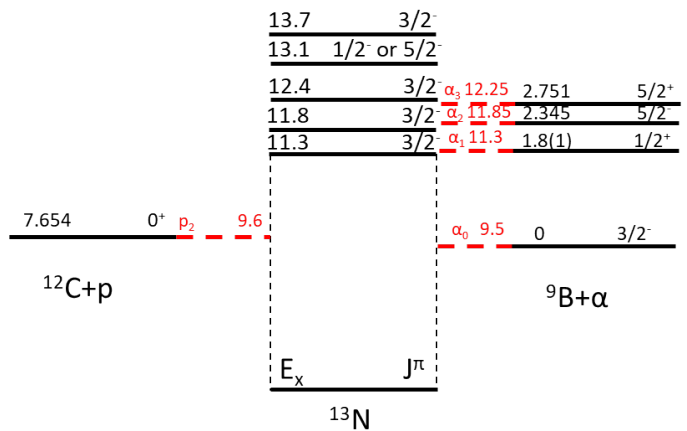


FIG. 4. Level scheme of measured  $3\alpha+p$  states in  ${}^{13}\text{N}$  in the central column with the proposed spin-parity assignments. The location of the thresholds for proton and  $\alpha$  decay are shown in red with the equivalent excitation energy shown. The corresponding states in the daughter nuclei ( ${}^{12}\text{C}$  and  ${}^9\text{B}$ ) are also shown.

cay via  $p+{}^{12}\text{C}(0_2^+)$  [ $p_2$ ],  $\alpha+{}^9\text{B}(g.s)$  [ $\alpha_0$ ],  $\alpha+{}^9\text{B}(\frac{1}{2}^+)$  [ $\alpha_1$ ] and  $\alpha+{}^9\text{B}(\frac{5}{2}^+)$  [ $\alpha_3$ ]. There is evidence of strength in  ${}^9\text{B}$  between 1 and 2.4 MeV excitation energy (Fig. 2). It is difficult to explain it without the  $\frac{1}{2}^+$  state in  ${}^9\text{B}$  [17] that is the mirror of the well-known  $\frac{1}{2}^+$  first excited state in  ${}^9\text{Be}$ . Attempts to fit the spectrum without the  $\frac{1}{2}^+$  in  ${}^9\text{B}$  fail because it is difficult to explain excess of counts at excitation energies between 1.4 and 2.4 MeV comparable to the 2.4 - 3.5 MeV region where there are known excited state in  ${}^9\text{B}$  states. Contributions from the broad 2.78 MeV  $\frac{1}{2}^-$  may give a signature similar to that seen albeit at lower energies (peaking at  $E_{rel} = 1.3$  MeV for a  ${}^{13}\text{N}(E_x) = 12.4$  MeV) when considering the expected yield from a  $\frac{1}{2}^-$  state in  ${}^{13}\text{N}$ . The  $L=0$   $\alpha$ -decay to the broad  $\frac{1}{2}^-$  in  ${}^9\text{B}$  will increase the yield at small excitation energies. While this possibility is disfavored from the observed spectrum due to the energy offset, it is mentioned here for completeness. The  $\frac{1}{2}^+$  state in  ${}^9\text{B}$  was selected by taking an excitation energy of between 1.4 and 2.4 MeV in  ${}^9\text{B}$  (following the centroid and width as observed via  ${}^9\text{Be}({}^3\text{He}, t)$  [17] which is consistent with our current results) and the  $\frac{5}{2}^+$  was taken as having an excitation energy of above 2.4 MeV. Any contribution from the relatively-narrow 2.345 MeV  $\frac{5}{2}^-$  is not present in the presented plots as this state decays almost exclusively via  ${}^5\text{Li}$  and therefore would not correspond to a peak in the  ${}^8\text{Be}$  spectrum. There were only 3 events associated with this decay to  ${}^5\text{Li}$  hence the statistics were insufficient to incorporate into the analysis.

Following the channel selection, the excitation energy in  ${}^{13}\text{N}$  was calculated and is shown in Fig. 5. Despite low statistics, a number of states can be seen and will be discussed individually. A summary of the properties of these

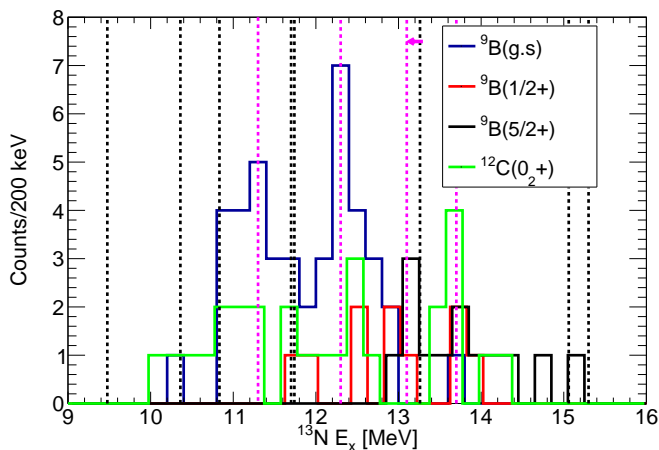


FIG. 5. Excitation spectrum in  $^{13}\text{N}$  for  $3\alpha + p$  separated by channels. Dashed vertical lines show previously-known states populated by  $\beta$ -decay in black and new states observed are shown in magenta. A magenta arrow shows a shift in the excitation energy between a suggested state at 13.26(10) MeV to 13.1(1) MeV.

states observed is then shown in Table I. A GEANT4 simulation was performed to test the variation in experimental resolution as a function of excitation energy for the  $\alpha_0$  channel which, is typically around  $\sigma = 200$  keV. The  $p_2$  channel resolution is almost entirely dominated by discrepancies between the calculated and real stopping powers for the  $\alpha$ -particles and therefore cannot be accurately determined. For all excitation energies, it is realistically greater than  $\sigma = 160$  keV.

### A. 11.3 MeV state

The first peak in the spectrum corresponds to an excitation energy of 11.3 MeV in  $^{13}\text{N}$ . The strength is almost entirely dominated by the  ${}^9\text{B}(\text{g.s.})+\alpha$  channel with a small fraction of  ${}^{12}\text{C}(0_2^+)+p$ . The yield in the  $p_0$  from the previous Knudsen data [11] shows a small, very narrow peak at the energy associated with this state ( $E_p(\text{lab}) = 8.64$  MeV) and is taken as 6(2.6). The yield in the  $p_1$  channel is harder to estimate due to the larger background from other states in this region but also shows no evidence of a peak and is also taken to be negligible. Fitting this peak in conjunction with neighboring peaks, the yield in the  $\alpha_0$  channel is 18(4.4) and yielding  $\sigma = 280(80)$  keV and  $E_x = 11.3(1)$  MeV. In the  $p_2$  channel, the yield is 7(2.8) with  $\sigma = 220(100)$  keV and  $E_x = 11.0(1)$  MeV. These widths are commensurate with the experimental resolution therefore  $\Gamma$  is expected to be relatively small ( $\Gamma < 200$  keV). Given the yields for  $\alpha_0$  and  $p_2$  are both strong, the spin-parity assignment is favored towards  $J^\pi = \frac{3}{2}^-$  where the angular momentum transfer is L=0 and L=1 respectively. A choice of  $J^\pi = \frac{1}{2}^-$  or  $J^\pi = \frac{5}{2}^-$  would require L=2 for the  $\alpha_0$  channel which

should heavily suppress the yield and  $J^\pi = \frac{5}{2}^-$  would correspond to L=3 for  $p_2$  so these options are strongly disfavored. From Table I, when taking the yield of the states and correcting for the different channel penetrabilities,  $P_L$ , and efficiencies, one can determine the structure of the measured states without a measurement of the width of the state to compare to the Wigner limit. Many of the states in  ${}^9\text{B}$  are very broad and the extreme simplification of calculating the penetrability to the resonant energy is made. In reality, the average penetrability will be higher. The structure is therefore determined by the fractional reduced-width,  $\bar{\gamma}_i^2 = \frac{\gamma_i^2}{\sum_j \gamma_j^2}$  where  $\gamma_i^2 = \frac{\Gamma_i}{2P_{iL}}$ . This variable shows the type of clustering but not the magnitude of the clustering. This state has considerable strength in both  $\alpha_0$  and  $p_2$  with  $\bar{\gamma}_i^2$  as 63% and 35% respectively. Taking the assumption that the total width,  $\Gamma$ , of the state is  $< 200$  keV, one may compare to the Wigner limit,  $\gamma_W^2 = \frac{\hbar^2}{\mu a^2}$  which is 0.57 and 2.1 MeV for  $\alpha$ -decay and  $p$ -decay respectively. Correspondingly, the ratio to Wigner,  $\theta_W^2 < 28\%$  and  $< 4\%$  for  $\alpha_0$  and  $p_2$  respectively. The former of these (while notably only an upper limit) constitutes a well-clustered state.

### B. 11.8 MeV state

In the  $p_2$  channel, the yield is 4(2.2) with  $\sigma = 170(110)$  keV and  $E_x = 11.8(1)$  MeV. Counts in the  $\alpha_1$  channel are from higher excitation energies extending down as the  $P_L$  for  $\alpha_1$  is extremely suppressed prohibiting any strength. Due to the strength of the two nearby states in the  $\alpha_0$  channel, the yield in the  $\alpha_0$  channel has very large uncertainties and can only be limited to be less than 1.8. There are two states previously known at this energy, a  $\frac{3}{2}^-$  and a  $\frac{5}{2}^-$  with widths of 115(30) and 530(80) keV respectively. Our data are more consistent with the narrower  $\frac{3}{2}^-$  which was also populated in previous work [11]. Additionally, a  $\frac{5}{2}^-$  assignment is the least favored from an angular momentum perspective (L=3 vs L=1 for  $\frac{1}{2}^-$  or  $\frac{3}{2}^-$ ) and this state is seen to populate the  $p_2$  channel reasonably well. From previous work, the yield in the  $p_0$  was determined to be 28(14). Making the same corrections for penetrabilities as above, this state shares strength in the  $p_0$  and  $p_2$  channels with  $\bar{\gamma}_i^2 > 51\%$  and  $> 39\%$  respectively with the remaining  $\alpha_0$  component being  $< 10\%$ . The width for this state is known and the reduced width for  $p_2$  can be compared to the Wigner limit and is  $\sim 1\%$ . Therefore, the contribution of the  ${}^{12}\text{C}(0_2^+) \otimes p$  configuration is small.

### C. 12.4 MeV state

Fitting this peak in conjunction with neighboring peaks, the yield in the  $\alpha_0$  channel is 22(4.8) and yielding  $\sigma = 310(90)$  keV and  $E_x = 12.4(1)$  MeV. The corre-

TABLE I. Excited states in  $^{13}\text{N}$  observed in this work with tentative spin-parity assignments, decay properties of the states, and the efficiency-corrected fractional reduced widths.

State		Counts						Efficiency-corrected $\bar{\gamma}^2$					
$E_x$	$J^\pi$	$\alpha_0$	$\alpha_1$	$\alpha_3$	$p_0$ [11]	$p_1$ [11]	$p_2$	$\alpha_0$	$\alpha_1$	$\alpha_3$	$p_0$	$p_1$	$p_2$
11.3(1)	3/2-	18(4.4)	0	0	6(2.6)	< 3	7(2.8)	67(21)%	0%	0%	4(2)%	<1%	29(13)%
11.8(1)	3/2-	< 1.8	0	0	28(14)	< 4	4(2.2)	<12%	0%	0%	50(30)%	0%	38(25)%
12.4(1)	3/2-	22(4.8)	4(2.2)	0	< 3	< 10	5(2.5)	6(2)%	88(49)%	0%	<0.1%	<2%	2(1)%
13.1	1/2-	0	3(2)	5(2.5)	21(6)	< 10	0	0%	1(1)%	98(48)% <sup>a</sup>	0%	<0.4%	0%
	5/2-							0%	10(10)%	89(44)%	0.7(0.2)%	<0.2%	0%
13.7(1)	3/2-	1(1.4)	3(2)	4(2.2)	< 3	< 10	6(2.7)	1(1)%	8(8)%	75(42)%	<0.5%	<7%	8(3)%

<sup>a</sup> Here the  $\alpha_3$  channel is assumed to be the  $J^\pi = \frac{1}{2}^-$  channel rather than the  $J^\pi = \frac{5}{2}^+$  state.

sponding yield of  $\alpha_1$  is 4(2.2). In the  $p_2$  channel, the yield is 5(2.5) with  $\sigma = 110(70)$  keV and  $E_x = 12.5(1)$  MeV. Despite the relatively small yield in the  $\alpha_1$  channel, when correcting for penetrability, the  $\alpha_1$  dominates the strength with  $\bar{\gamma}_i^2 = 91\%$  with  $\alpha_0$  and  $p_2$  sharing the remainder with 6% and 3% respectively. The strong contribution of the  ${}^9\text{B}(\frac{1}{2}^+) \otimes \alpha$  configuration suggests this is a near-threshold p-wave state.

The  ${}^9\text{Be}(\alpha, \alpha_0)$  [18, 19] and  ${}^9\text{Be}(\alpha, n_0)$  [20] reactions data are available at this excitation energy and above and one may look for analogous states in  $^{13}\text{C}$ . Given this state is in the s-wave in the entrance channel (assuming  $J^\pi = \frac{3}{2}^-$ ) and is expected to be relatively narrow, and previous data seem to have a very large experimental width, it is perhaps possible to explain that such a state has not been observed in  $^{13}\text{C}$  in the  ${}^9\text{Be}(\alpha, \alpha_0)$  channel. The sole dominant feature in this region is a strong  $\frac{5}{2}^+$  state at 11.95 MeV.

It is worth noting that the  $\alpha_1$  channel is sub-threshold in  $^{13}\text{C}$  and the  $n_2$  channel is heavily-suppressed until  $^{13}\text{C}$  excitation energies of above 13 MeV [20]. There are many states in this region ( $E_\alpha > 2$  MeV) visible in the  ${}^9\text{Be}(\alpha, n_0)$  channel but the resolution is insufficient to provide spin-parity and width assignments.

This perhaps motivates a more extensive investigation of near-threshold states in  $^{13}\text{C}$  from the  ${}^9\text{Be} + \alpha$  channel with higher resolution and angular coverage. It is also worth noting that in the previous proton data [11] there is a peak at this corresponding energy for the  $p_1$  channel ( $E_p(\text{lab}) = 5.55$  MeV) where a peak with a yield of  $\approx 6$  can be seen above a considerable background. The conservative limit of  $< 10$  for  $p_1$  is therefore taken. The width in this spectrum is also seen to be small which agrees with our results.

#### D. 13.1 MeV state

A relatively strong peak is seen at 13.1 MeV in the  $\alpha_3$  channel where decays occur through the 2.75 MeV  $\frac{5}{2}^+$ . There is only a very small contribution from the  $\alpha_1$  channel at this excitation energy so this state is almost

exclusively  ${}^9\text{B}(\frac{5}{2}^+) \otimes \alpha$ . Given the dominance of  $\alpha_3$ , this suggests a spin-parity of  $J^\pi = \frac{5}{2}^-$  which suppresses the other channels.

In  ${}^9\text{B}$ , there is also the extremely-broad 2.78 MeV  $\frac{1}{2}^-$  with  $\Gamma = 3.13$  MeV which may actually be the source of the  $\alpha_3$  strength. Our data do not have sufficient statistics to exclude this possibility and the  $\frac{1}{2}^-$  decays primarily through  ${}^8\text{Be}$  via proton-decay. In this possibility, the preferred spin-parity assignment is obviously  $J^\pi = \frac{1}{2}^-$  corresponding to L=0  $\alpha_3$  decay. The results for both spin parities assignments are included in Table I.

As with the 12.4 MeV state, there is evidence of a peak in previous data at the correct energy in the  $p_1$  channel ( $E_p(\text{lab}) = 6.20$  MeV) which is given a similar limit of  $< 10$ .

#### E. 13.7 MeV state

There is a collection of strength in the  $p_2$ ,  $\alpha_0$ ,  $\alpha_1$  and  $\alpha_3$  channel. With a yield of 6(2.7), the state is dominated by  $p_2$  and has parameters of  $\sigma = 260(70)$  keV and  $E_x = 13.7(1)$  MeV. Given the small yield in the  $\alpha_3$ , this state can be assigned as either  $\frac{3}{2}^-$  or  $\frac{5}{2}^-$ . A  $\frac{5}{2}^-$  would correspond to L=3 for the  $p_2$  channel so a  $\frac{3}{2}^-$  assignment would be more commensurate with the reasonable  $p_2$  yield. This state also exhibits a  ${}^9\text{B}(\frac{5}{2}^+) \otimes \alpha$  structure.

Examining the previous work for evidence of a peak in the  $p_1$  is not possible for this state due to the presence of a strong  $p_0$  branch from a lower-lying state at the same energy. A similar limit of  $< 10$  is therefore placed on this state.

## V. CONCLUSIONS

$\beta$ -delayed  $3\alpha\text{p}$  decay has been observed for the first time. While  $\beta$ -delayed  $\alpha\text{p}$  has been previously observed in  ${}^9\text{C}$  [21],  ${}^{17}\text{Ne}$  [22],  ${}^{21}\text{Mg}$  [23] and  ${}^{23}\text{Si}$  [24], these states did not provide any structural insight and instead were mainly seen through isobaric analogue states that were

well fed by  $\beta$ -decay. In this work,  $\beta 3\alpha p$  decay was observed from the states below the isobaric analog in  $^{13}\text{N}$  at  $E_x = 15$  MeV, demonstrating this is not merely a phase-space effect. The  $\beta$ -delayed  $3\alpha p$  decays observed here are in strong competition with  $\beta$ -delayed proton decay and therefore the states must have significant clustering.

Three new states and a previously-tentative state in  $^{13}\text{N}$  have been observed with a strong  $3\alpha + p$  nature. The first is a narrow  $\frac{3}{2}^-$  state at  $E_x = 11.3(1)$  MeV with mixed  ${}^9\text{B}(\text{g.s.}) \otimes \alpha$  and  $p + {}^{12}\text{C}(0_2^+)$  nature.

Another previously-observed  $\frac{3}{2}^-$  was seen to have mixed  $p + {}^{12}\text{C}(\text{g.s.})$  and  $p + {}^{12}\text{C}(0_2^+)$  nature at 11.8 MeV with around half of the total strength as  $p + {}^{12}\text{C}(\text{g.s.})$ .

At higher excitation, another strong  $\alpha$ -decaying state was seen at  $E_x = 12.4(1)$  MeV although this state has a much stronger  ${}^9\text{B}(\frac{1}{2}^+) \otimes \alpha$  nature.

A revised excitation energy of 13.1(1) MeV is suggested for a previously-seen state at 13.26 MeV. The  ${}^9\text{B}(\frac{5}{2}^+) \otimes \alpha$  structure dominates in this state and a spin assignment of  $J^\pi = \frac{1}{2}^-$  or  $\frac{5}{2}^-$  are therefore preferred.

Finally, another  $\frac{3}{2}^-$  is seen at 13.7 MeV which is also dominated by  ${}^9\text{B}(\frac{5}{2}^+) \otimes \alpha$ .

The inability to extract the width of these narrow states means that the magnitude of clustering cannot be fully evaluated, however, the type (channel) of clustering can be determined without this information. Higher res-

olution data focusing on the proton channel may provide further information on the magnitude of this clustering phenomenon. From our current data, one may conclude that the clustered channels are competitive against the single-particle  $p_0$  channel, highlighting the importance of cluster configurations in non-self-conjugate nucleus  $^{13}\text{N}$ .

Evidence for the low-lying  $\frac{1}{2}^+$  in  ${}^9\text{B}$  in these background-free data, matching the parameters of previous observations [17], brings us closer to resolving the long-standing problem of searches for this elusive state.

## VI. ACKNOWLEDGMENTS

We thank Vlad Goldberg for helpful feedback on this work. This work was supported by the U.S. Department of Energy, Office of Science, Office of Nuclear Science under Award No. DE-FG02-93ER40773 and by the National Nuclear Security Administration through the Center for Excellence in Nuclear Training and University Based Research (CENTAUR) under Grant No. DE-NA0003841. G.V.R. also acknowledges the support of the Nuclear Solutions Institute. S.A., S.M.C., C.K., D.K., S.K. and C.P. also acknowledge travel support from the IBS grant, funded by the Korean Government under grant number IBS-R031-D1. C.N.K acknowledges travel support from the National Research Foundation of Korea (NRF) grant, funded by the Korea government (MSIT) (No. 2020R1A2C1005981 and 2013M7A1A1075764).

- 
- [1] M. Pfützner, M. Karny, L. V. Grigorenko, and K. Riisager, *Rev. Mod. Phys.* **84**, 567 (2012).
- [2] B. Blank and M. Płoszajczak, *Reports on Progress in Physics* **71**, 046301 (2008).
- [3] M. Seya, M. Kohno, and S. Nagata, *Progress of Theoretical Physics* **65**, 204 (1981), <https://academic.oup.com/ptp/article-pdf/65/1/204/5250151/65-1-204.pdf>.
- [4] W. von Oertzen, *Zeitschrift für Physik A Hadrons and Nuclei* **354**, 37 (1996).
- [5] Y. Kanada-En'yo, M. Kimura, and A. Ono, *Progress of Theoretical and Experimental Physics* **2012** (2012), 10.1093/ptep/pts001, 01A202, <https://academic.oup.com/ptep/article-pdf/2012/1/01A202/11578300/pts001.pdf>.
- [6] W. von Oertzen, H. G. Bohlen, M. Milin, T. Kokalova, S. Thummerer, A. Tumino, R. Kalpakchieva, T. N. Massey, Y. Eisermann, G. Graw, T. Faestermann, R. Hertenberger, and H.-F. Wirth, *The European Physical Journal A - Hadrons and Nuclei* **21**, 193 (2004).
- [7] M. Milin and W. von Oertzen, *The European Physical Journal A - Hadrons and Nuclei* **14**, 295 (2002).
- [8] H. Yamaguchi, D. Kahl, S. Hayakawa, Y. Sakaguchi, K. Abe, T. Nakao, T. Suhara, N. Iwasa, A. Kim, D. Kim, S. Cha, M. Kwag, J. Lee, E. Lee, K. Chae, Y. Wakabayashi, N. Imai, N. Kitamura, P. Lee, J. Moon, K. Lee, C. Akers, H. Jung, N. Duy, L. Khiem, and C. Lee, *Physics Letters B* **766**, 11 (2017).
- [9] M. Barbui, A. Volya, E. Aboud, S. Ahn, J. Bishop, V. Z. Goldberg, J. Hooker, C. H. Hunt, H. Jayatissa, T. Kokalova, E. Koshchiy, S. Pirrie, E. Pollacco, B. T. Roeder, A. Saastamoinen, S. Upadhyayula, C. Wheldon, and G. V. Rogachev, *Phys. Rev. C* **106**, 054310 (2022).
- [10] A. Volya, M. Barbui, V. Z. Goldberg, and G. V. Rogachev, *Communications Physics* **5**, 322 (2022).
- [11] H. H. Knudsen, H. O. U. Fynbo, M. J. G. Borge, R. Boutami, P. Dendooven, C. A. Diget, T. Eronen, S. Fox, L. M. Fraile, B. Fulton, J. Huikary, H. B. Jeppesen, A. S. Jokinen, B. Jonson, A. Kankainen, I. Moore, A. Nieminen, G. Nyman, H. Penttilä, K. Riisager, S. Rinta-Antila, O. Tengblad, Y. Wang, K. Wilhelmssen, and J. Äystö, *Phys. Rev. C* **72**, 044312 (2005).
- [12] J. Bishop, G. V. Rogachev, S. Ahn, E. Aboud, M. Barbui, A. Bosh, C. Hunt, H. Jayatissa, E. Koshchiy, R. Malecek, S. T. Marley, E. C. Pollacco, C. D. Pruitt, B. T. Roeder, A. Saastamoinen, L. G. Sobotka, and S. Upadhyayula, *Phys. Rev. C* **102**, 041303 (2020).
- [13] J. Bishop, G. Rogachev, S. Ahn, E. Aboud, M. Barbui, P. Baron, A. Bosh, E. Delagnes, J. Hooker, C. Hunt, H. Jayatissa, E. Koshchiy, R. Malecek, S. Marley, R. O'Dwyer, E. Pollacco, C. Pruitt, B. Roeder, A. Saastamoinen, L. Sobotka, and S. Upadhyayula, *Nuclear Instruments and Methods in Physics Research Section A: Accelerators, Spectrometers, Detectors and Associated Equipment* **964**, 163773 (2020).

- [14] R. Tribble, R. Burch, and C. Gagliardi, Nuclear Instruments and Methods in Physics Research Section A: Accelerators, Spectrometers, Detectors and Associated Equipment **285**, 441 (1989).
- [15] E. Pollacco, G. Grinyer, F. Abu-Nimeh, T. Ahn, S. Anvar, A. Arokiaraj, Y. Ayyad, H. Baba, M. Babo, P. Baron, D. Bazin, S. Beceiro-Novo, C. Belkhiria, M. Blaizot, B. Blank, J. Bradt, G. Cardella, L. Carpenter, S. Ceruti, E. D. Filippo, E. Delagnes, S. D. Luca, H. D. Witte, F. Druillolle, B. Duclos, F. Favela, A. Fritsch, J. Giovinazzo, C. Gueye, T. Isobe, P. Hellmuth, C. Huss, B. Lachacinski, A. Laffoley, G. Lebertre, L. Legeard, W. Lynch, T. Marchi, L. Martina, C. Maugeais, W. Mittig, L. Nalpas, E. Pagano, J. Pancin, O. Poleshchuk, J. Pedroza, J. Pibernat, S. Primault, R. Raabe, B. Raine, A. Rebi, M. Renaud, T. Roger, P. Roussel-Chomaz, P. Russotto, G. Saccà, F. Saillant, P. Sizun, D. Suzuki, J. Swartz, A. Tizon, N. Usher, G. Wittwer, and J. Yang, Nuclear Instruments and Methods in Physics Research Section A: Accelerators, Spectrometers, Detectors and Associated Equipment **887**, 81 (2018).
- [16] J. Holmes, E. Galyaev, R. Alarcon, R. Acuna, D. Blyth, B. Fox, N. Mullins, and K. Scheuer, Journal of Instrumentation **15**, T05001 (2020).
- [17] C. Wheldon, T. Kokalova, M. Freer, J. Walshe, R. Hertenberger, H.-F. Wirth, N. I. Ashwood, M. Barr, N. Curtis, T. Faestermann, R. Lutter, J. D. Malcolm, and D. J. Marín-Lámbarri, Phys. Rev. C **91**, 024308 (2015).
- [18] J. D. Goss, S. L. Blatt, D. R. Parsignault, C. D. Porterfield, and F. L. Riffle, Phys. Rev. C **7**, 1837 (1973).
- [19] Lombardo, Ivano, Dell'Aquila, Daniele, and Vigilante, Mariano, EPJ Web Conf. **165**, 01036 (2017).
- [20] A. W. Obst, T. B. Grandy, and J. L. Weil, Phys. Rev. C **5**, 738 (1972).
- [21] E. Gete, L. Buchmann, R. E. Azuma, D. Anthony, N. Bateman, J. C. Chow, J. M. D'Auria, M. Dombbsky, U. Giesen, C. Iliadis, K. P. Jackson, J. D. King, D. F. Measday, and A. C. Morton, Phys. Rev. C **61**, 064310 (2000).
- [22] J. C. Chow, J. D. King, N. P. T. Bateman, R. N. Boyd, L. Buchmann, J. M. D'Auria, T. Davinson, M. Dombbsky, E. Gete, U. Giesen, C. Iliadis, K. P. Jackson, A. C. Morton, J. Powell, and A. Shotter, Phys. Rev. C **66**, 064316 (2002).
- [23] M. Lund, M. Borge, J. Briz, J. Cederkäll, H. Fynbo, J. Jensen, B. Jonson, K. Laursen, T. Nilsson, A. Perea, V. Pseudo, K. Riisager, and O. Tengblad, Physics Letters B **750**, 356 (2015).
- [24] A. A. Ciemny, C. Mazzocchi, W. Dominik, A. Fijałkowska, J. Hooker, C. Hunt, H. Jayatissa, L. Janiak, G. Kamiński, E. Koshchiy, M. Pfützner, M. Pomorski, B. Roeder, G. V. Rogachev, A. Saastamoinen, S. Sharma, N. Sokołowska, W. Satuła, and J. Singh, Phys. Rev. C **106**, 014317 (2022).